

Chapter 5

Saturation and Capillary Pressure



5.1 Saturation

Saturation is defined as the ratio of the fluid volume in the porous medium to the pore volume of the rock. That means, saturation is the proportion of interrelated aperture full by a specified phase. For a gas-oil-water system. Therefore, the following formulas show the saturation ratio for every single phase in the porous medium (Eqs. 5.1–5.4):

$$S_w = \frac{V_w}{V_p} \tag{5.1}$$

$$S_o = \frac{V_o}{V_p} \tag{5.2}$$

$$S_g = \frac{V_g}{V_p} \tag{5.3}$$

$$S_w + S_o + S_g = 1 \tag{5.4}$$

where:

S_w = water saturation

S_o = oil saturation

S_g = gas saturation

5.2 Determination of Fluid Saturation from Rock Sample

There are two available techniques used to determine rock saturation. The first method applied is by evaporating the fluids in the rock and the second method is by extracting the fluids out of the rock using solvent. The following are the applied techniques:

1. Retort method

In this method placed the core sample at high temperature to vaporize all the fluids in the core plug (water and oil). Then, collect these condensed fluids in a vessel and measure the saturation for every single liquid. There are a few disadvantages to using this method. For instance, the method needs high temperature to vaporize all the oil in the core plug (1100 °F), this will drive the water as well causing water recovery values more than just interstitial water. Also, at high temperature the oil tends to cack and crack. Consequently, the test results need to be corrected before use.

2. ASTM method

This approach is relying on the extracting the liquids from the core sample by using solvent. The core sample is sited and vapor of either toluene, gasoline, or naphtha goes through the core plug and is condensed to inflow back over the core plug. This procedure leaks out liquids in the sample see Fig. 5.1. The experiment continues until no additional water is collected in the graduated tube. After complete the experiment, water saturation can be measured directly, while for oil saturation can be measured by deducting the core plug weight before the test, the dried core weight after the test, and the extracted water weight.

Fig. 5.1 Dean-Stark apparatus



5.3 Reservoir Saturation with Depth

The key significance of capillary pressure is its influence on the distribution of fluids in the reservoir along with the depth. For every phase (k), reservoir pressure rises with depth (z) dependent on phase density (Eqs. 5.5–5.10):

$$\frac{dp_k}{dz} = \rho_k g \quad (5.5)$$

and since,

$$P_o - P_w = P_{cow} \quad (5.6)$$

$$\frac{dP_{cow}}{dz} = -(\rho_o - \rho_w) \cdot g \quad (5.7)$$

Therefore

$$\frac{\Delta P_{cow}}{\Delta z} = -(\rho_o - \rho_w) \cdot g \quad (5.8)$$

if Δz = width of the transition zone, where

$$\Delta P_{cow} = P_{cow}(S_o = 1 - S_{wc}) - P_{cow}(S_o = 0) \quad (5.9)$$

But

$$P_{cow}(S_o = 0) = 0$$

so that

$$\Delta z = -\frac{P_{cow}(S_o = 1 - S_{wc})}{(\rho_o - \rho_w) \cdot g} \quad (5.10)$$

High permeability at about 90° contact angle systems results in small capillary pressures, resulting in smaller transition zone. However, low permeability with small contact angle systems will result large capillary pressures and wide transition zones. Figure 1.11 displays a diagram for an oil-water reservoir of oil and water pressures versus depth (right-hand plot) and of oil/water capillary pressure versus water saturation (left-hand plot). Initially, the reservoir has been saturated with water ($S_w = 100\%$). After that, oil migrated and displaced water from the reservoir shown in Fig. 5.2.

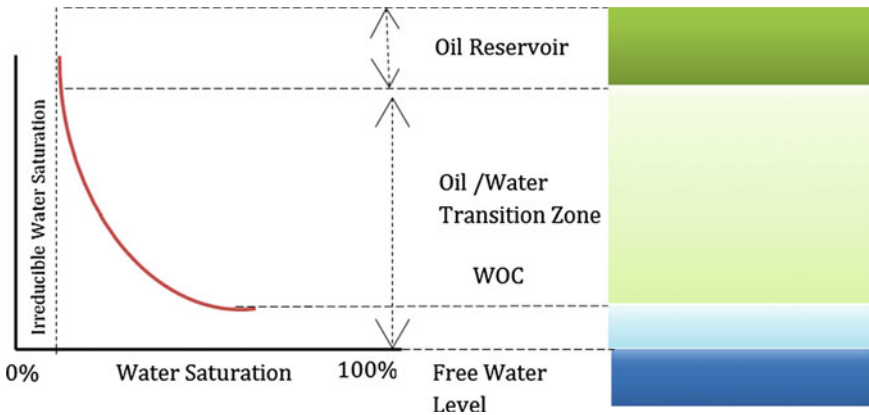


Fig. 5.2 Water saturation versus capillary pressure with diagram of oil-water capillary transition zone

5.4 Capillary Pressure

The combination of the impact of the surface and interfacial tensions of the reservoir fluids, the aperture size and shape, and the wetting features of the system will generate capillary forces in hydrocarbon reservoir (two immiscible fluids available in the aperture of the reservoir rock). Usually, one phase defined as a wetting phase and the other phase defined as a non-wetting phase. When both fluids are in contact, a discontinuity in pressure present between the two immiscible fluids, which rely on the curvature of the interface splitting the fluids. This pressure difference identified as capillary pressure (P_c).

The aperture size can be determined using mercury capillary pressure curves, that are obtained by injecting mercury (non-wetting phase) into a core sample containing air (wetting phase). The mercury injected with increasing pressure and a plot of injection pressure versus the volume of mercury injected (H_g saturation) see Fig. 5.3. The Hg saturation plotted versus bulk volume or pore volume. The curve is known as the drainage curve shown in Fig. 5.3a. If the injection pressure is decreased wetting phase, either air or water will flow inside the aperture and the non-wetting fluid will be expelled (Kolodizie 1980). This method is called imbibition, and a plot of pressure versus saturation is identified as the imbibition curve see Fig. 5.3b.

The capillary pressure data are needed for three key uses:

- The calculation of initial reservoir fluid saturations.
- Cap-rock seal capacity.
- As additional data for evaluation of relative permeability data.

Pore-throat size is known as the aperture size that connects the bigger apertures. It depends on the idea that the inter-particle aperture can be envisioned as spaces with connecting gates (Swanson 1981). The gates are the pore-throats that connect the larger apertures, or spaces.

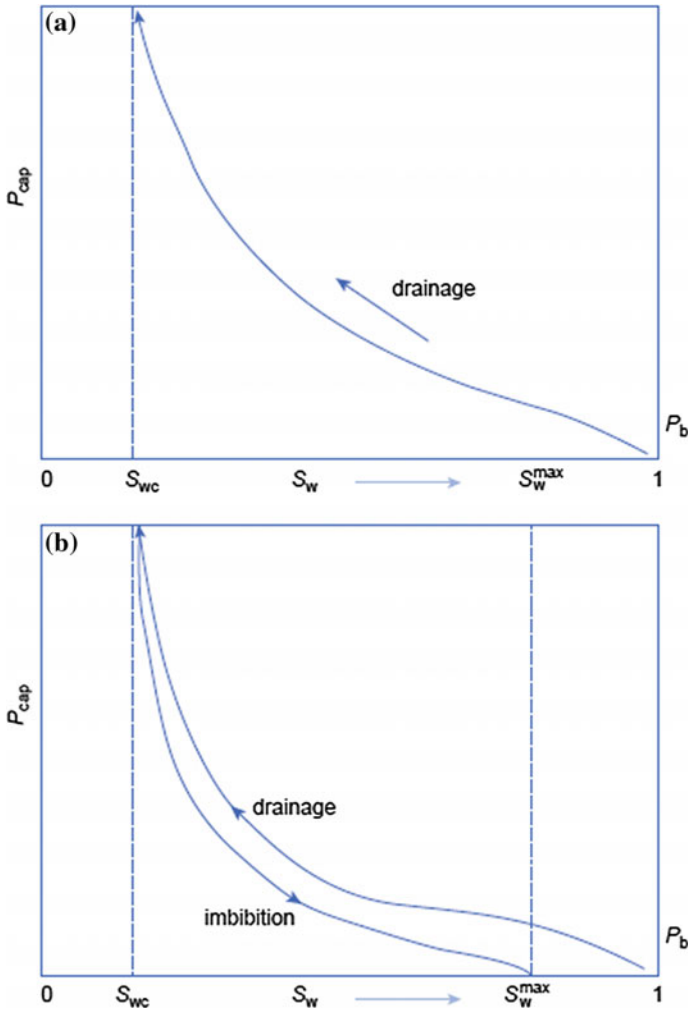


Fig. 5.3 Capillary pressure versus water saturation. **a** Drainage capillary pressure curve. **b** Drainage and imbibition capillary pressure curves

The fundamental relationship depicted in Figs. 5.4 and 5.5 between capillary pressure, aperture radius, interfacial tension, and the contact angle is expressed by Eq. 5.11. Figure 5.4 showing a three-phase water-wet system (water-oil-rock) at equilibrium. The curvature of the interfacial boundary is deepening on of interstitial volume, grain size, fluid saturation, and surface tension. The contact angle (θ) is a depend on the relative wetting characteristics of the two fluids with respect to the solid.

$$P_c = \frac{2\sigma \cos \theta}{r} \cdot A \tag{5.11}$$

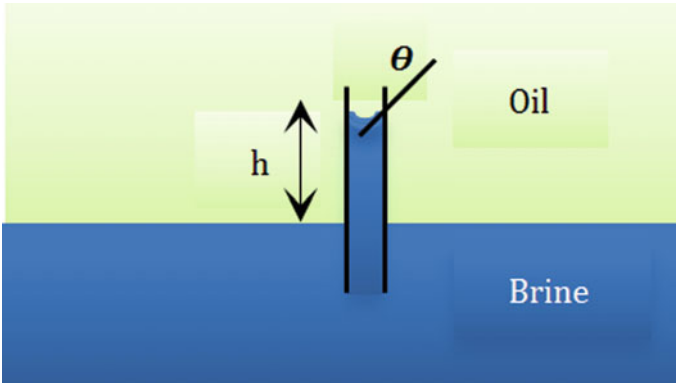
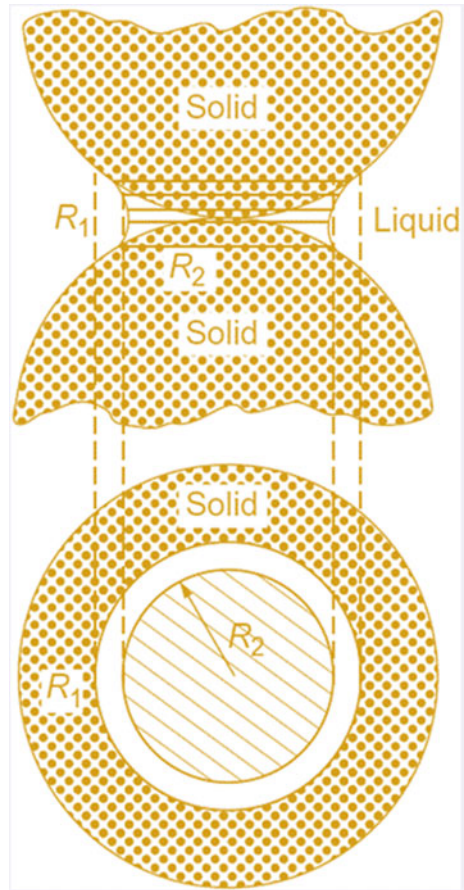


Fig. 5.4 Capillary pressure definitions

Fig. 5.5 Diagram showing radii of interfacial curvature at equilibrium for the three-phase system (oil-water-rock)



where:

- P_c = Capillary pressure (psi)
- σ = Interfacial tension (dynes/cm)
- θ = Contact angle (degrees)
- r = Radius of the pore throat (microns)
- $A = 145 \times 10^{-3}$ (constant to convert to psi)

Identifying the wetting fluid pressure by p_w and non-wetting fluid pressure by p_{nw} , the capillary pressure can be presented as Capillary pressure = (pressure of the non-wetting phase) – (pressure of the wetting phase). The Capillary pressure can be defined as (Eq. 5.12):

$$P_c = (\rho_{nw} - \rho_w)gh = \frac{2\sigma \cos \theta}{r} \cdot A \tag{5.12}$$

where:

- ρ_{nw} = Density of Non-wetting phase, (lb/ft³)
- ρ_w = Density of wetting phase, (lb/ft³)
- g = Acceleration, (ft/sec²)
- h = Capillary rise, (ft)

Typical Values for changing mercury/air/oil/water capillary pressure curves to reservoir conditions of gas/oil/water are specified in Table 5.1.

Figure 5.6 illustrations some cases for sandstone formation that has almost the same porosity with different permeability.

- Core A: porosity $\phi = 0.216$, permeability $k = 430$ mD
- Core B: porosity $\phi = 0.220$, permeability $k = 116$ mD
- Core C: porosity $\phi = 0.196$, permeability $k = 13.4$ mD

Table 5.1 Capillary Pressure Properties at reservoir and laboratory conditions for Different types of Fluid

System	θ	σ		$\sigma \cdot \cos \theta$	
		Dynes cm^{-1}	N $\text{cm}^{-1} = P_{am}$	Dynes cm^{-1}	N $\text{cm}^{-1} = P_{am}$
<i>Laboratory</i>					
Air-water	0	72	0.072	72	0.072
Oil-water	30	48	0.048	42	0.042
Air-mercury	40	480	0.480	367	0.367
Air-oil	0	24	0.024	24	0.024
<i>Reservoir</i>					
Water-oil	30	30	0.030	26	0.026
Water-gas	0	50	0.050	50	0.050

Source Hartmann and Beaumont (1999) and Darling (2005)

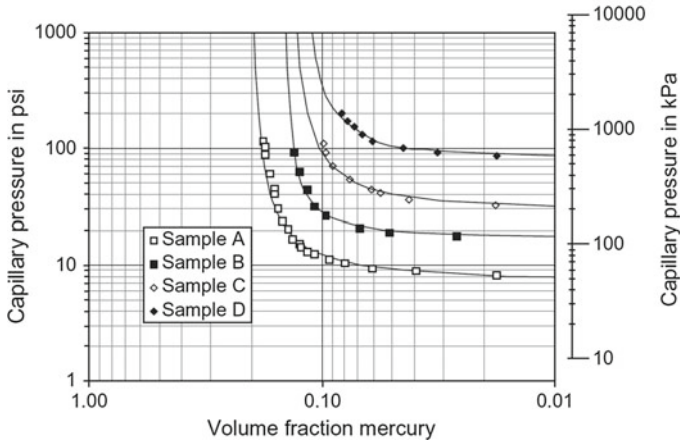


Fig. 5.6 Capillary pressure curves from a sandstone reservoir. *Source* Archie (1950) and Jorden and Campbell (1984)

Core D: porosity $\emptyset = 0.197$, permeability $k = 1.2$ mD.

The figure exhibits the effect of pore radius on the permeability and capillary pressure. Where at large pore throat diameter, the results show high permeability and low capillary pressure. Conversely, at small pore throat diameter the results show low permeability and high capillary pressure. The conclusion of the capillary pressure curve functions is:

1. Defines the fluid saturation diffusion in a reservoir rock, which reliant on the pore size distribution and wettability of the fluid mechanisms.
2. Characterizes the fluid dispersion as a function of pressure.
3. Indicate the largest pores in the reservoir rock, from displacement pressure, which control the permeability.
4. Obtain both, irreducible water saturation and residual oil saturation;
5. Provide good indication for the distribution of the pore size in the reservoir rock.

Usually, the capillary pressure is a function of the height above the free water level (FWL). Therefore, when the capillary pressure curve and the FWL are known, then it becomes simple to determine the water saturation at any depth in the reservoir see Fig. 5.7. If water saturation value for a given well is matched with the estimated water saturations from wireline tools and core, the wireline water saturation value can be applied in the other reservoir section where no cores are available within the same field.

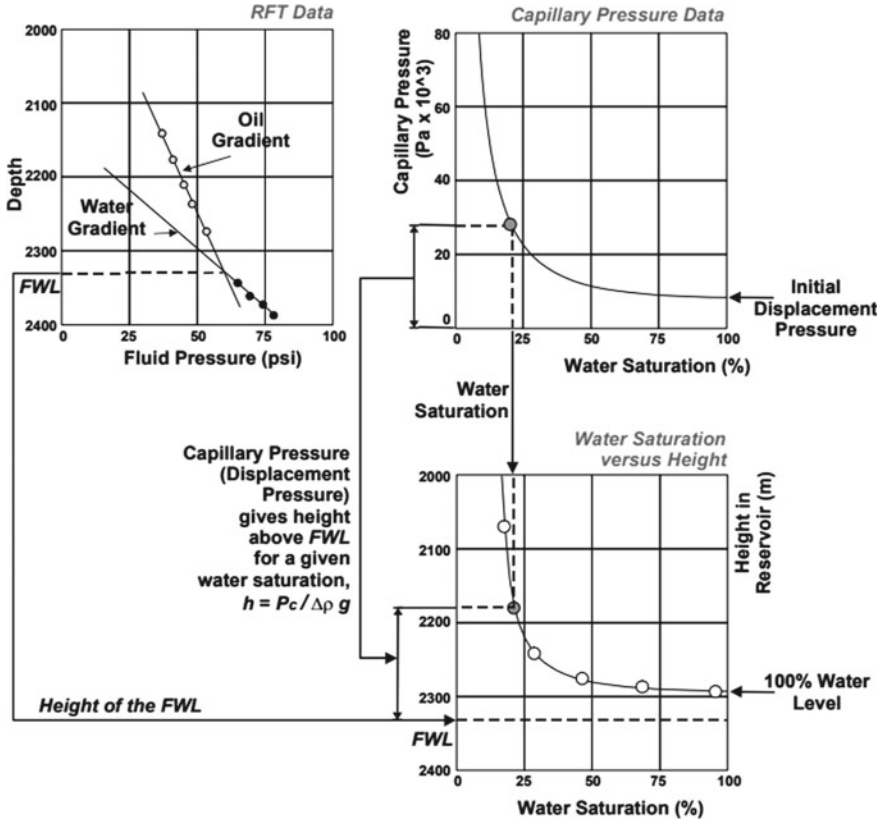


Fig. 5.7 Determination of water saturation in a reservoir

5.5 Laboratory Methods of Measuring Capillary Pressure

There are three main approved techniques to measure capillary pressures in the laboratory are:

1. Mercury Injection Method
2. Porous plate Diaphragm (or restored state) Method
3. Centrifugal Method

Typically, these techniques carried out in the laboratory using core samples from reservoir. There are so many factors and process that affect or alter the initial condition of the core sample such as drilling and coring fluids, coring method, core handling, and transportation, packing and experimental procedures. Consequently, special cares are required to prevent changing the initial core condition. In case of altering the initial core conditions due to any of the upper mentioned reasons, the core must be restored to its initial condition before conducting capillary pressure test.

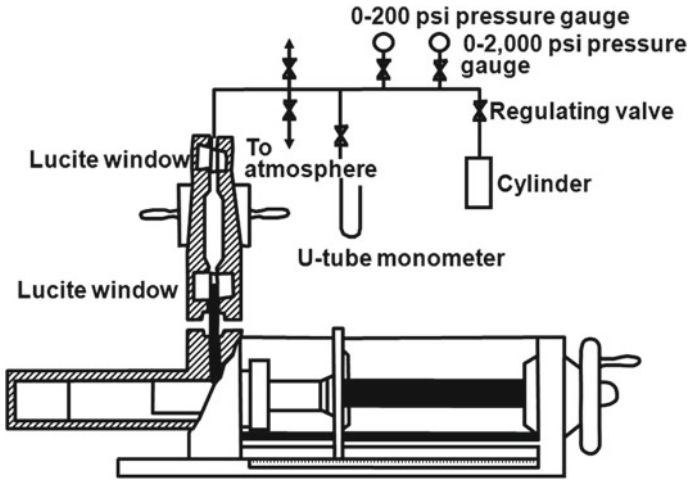


Fig. 5.8 Mercury injection apparatus

1. Mercury Injection Method

Commonly, this method used cleaned and dried core samples. the Mercury Injection procedures are as following:

1. Place the core in a chamber and immersing the core sample in Mercury at $<10^{-3}$ mm H_g and evacuate the core within the mercury injection apparatus showing in Fig. 5.8.
2. Inject the mercury in the core sample.
3. The mercury volume that has filled the pores at each forced pressure can be measured from volumetric readings, and the Mercury entered the pore space can be calculated.
4. Additional readings can be obtained as the pressure is dropped to provide data for the imbibition case from S_{wi} to $P_c = 0$.
5. Continue for several pressures and plot the pressure against the mercury saturation.

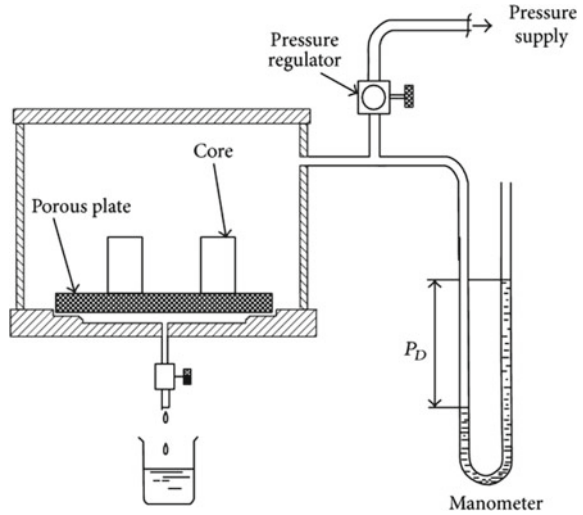
Usually, to convert to oil-brine or gas-brine data using suitable contact angles and interfacial tensions. General conversions are given below (Eqs. 5.13–5.16):

$$P_C(\text{gas-brine}) = P_C(\text{Air-Hg}) \frac{72 \cos 0^\circ}{480 \cos 130^\circ} \tag{5.13}$$

$$P_C = 0.233 P_C(\text{Air-Hg}) \tag{5.14}$$

$$P_C(\text{oil-brine}) = P_C(\text{Air-Hg}) \frac{25 \cos 0^\circ}{480 \cos 130^\circ} \tag{5.15}$$

Fig. 5.9 Porous plate apparatus



$$P_C = 0.070 P_C(\text{Air-Hg}) \tag{5.16}$$

The non-wetting phase saturation can be obtained by dividing the volume of mercury injected by the pore volume. In the experiment, the capillary pressure is injection pressure. This method can be conducted very fast, and there is no pressure limitation. The method can only be applied for shaped cores.

2. Porous Diaphragm Method

Porous plate method used a core sample saturated totally with a wetting fluid. The experimental procedures are stated as follows:

1. Saturate the core plug and the Porous plate with the fluid to be displaced.
2. Place the core on a porous plate as shown in Fig. 5.9).
3. Use a different level of pressure (e.g. 1, 2, 4, 8, 16, 32, 64 psi), wait for the core to reach static equilibrium. In the end, a capillary pressure curve can be plotted against water saturation in the sample shown in Fig. 5.10. To reach the equilibrium, it takes from 10 to 40 days.

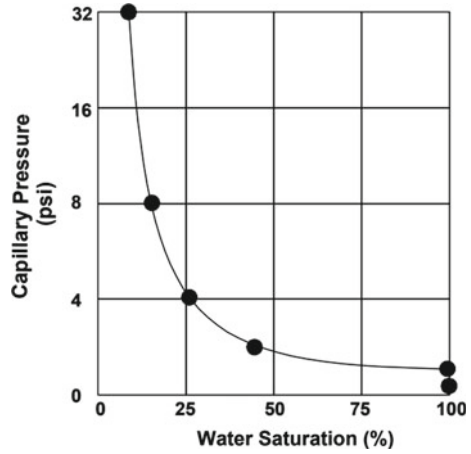
The capillary pressure = height of liquid column + applied pressure

$$\textit{Saturation} = \frac{\textit{Pore Voulme} - \textit{Colume Produced}}{\textit{Pore Voulme}} \tag{5.17}$$

3. Centrifugal Method

This method uses a core sample of 100% saturated with a wetting fluid. The main centrifugal method procedures are as the following:

Fig. 5.10 Capillary pressure measurements using porous plate



1. The core sample placed in the core holder in the centrifuge depicted in Fig. 5.11 and rotates at a fixed constant speed. The speed of rotation causes a centripetal force displaces some wetting fluid, which can be determined at the window using a stroboscope. Also, the saturation can be obtained. At low rotation speeds, the centripetal force is only displacing water from the biggest pores. However, at higher speeds, the centripetal force is capable to displace water from very smaller pores in the core plug.
2. The rotary motion of the centrifuge is converted to capillary pressure using appropriate equations.
3. Repeat for several speeds and plot capillary pressure with saturation refer to Fig. 5.12.

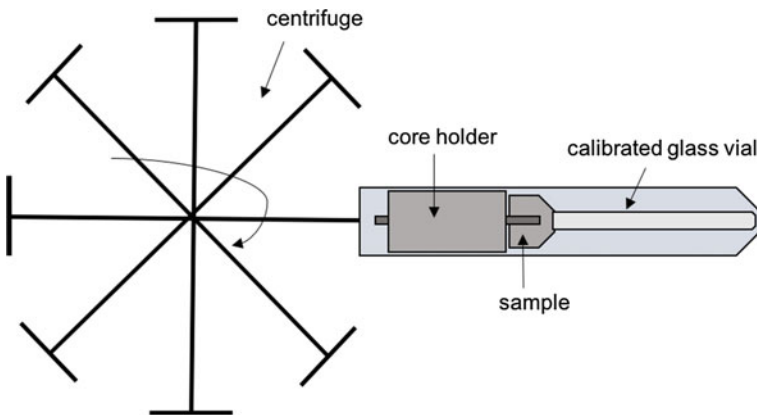
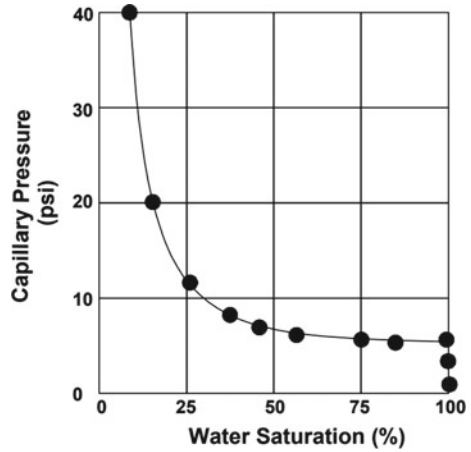


Fig. 5.11 A schematic of a centrifuge set-up for determining capillary pressure

Fig. 5.12 Capillary pressure measurements using centrifuge apparatus



5.6 Capillary Hysteresis

Correct measurements of capillary pressure and relative permeability are very significant for assessing oil and gas recovery methods. Besides, resistivity index parameters are very significant in estimating fluid diffusion in reservoirs. The different in drainage and imbibition processes, generally known as hysteresis. Therefore, the hysteresis phenomenon is known as the equilibrium situations of the air-water interfaces in a system of pores are reliant on water content in the system is increasing or decreasing.

5.7 Averaging Capillary Pressure Data: Leverett J-Function

Normally, the capillary pressure measurements are obtained on small core samples that characterize small section of the reservoir. Consequently, it is required to use all obtained capillary pressure data to describe a given reservoir.

Typically, there are different capillary pressure-saturation curves for many reservoir rock types that have various features see Fig. 5.13. Therefore, a common equation to describing all such curves was developed by Leverett (1941). Initially, Leverett converted all capillary pressure data to a general curve. However, a general capillary pressure curve does not available as the rock properties have big variation with rock type.

Leverett noticed that capillary pressure is dependent on porosity, permeability, interfacial tension, and pore radius. Leverett presented his equation as dimensionless equation which called “J-function ($J(S_w)$)” and it is function of saturation (Eq. 5.18). Actually, J-function is away to extrapolating capillary pressure data for a particular

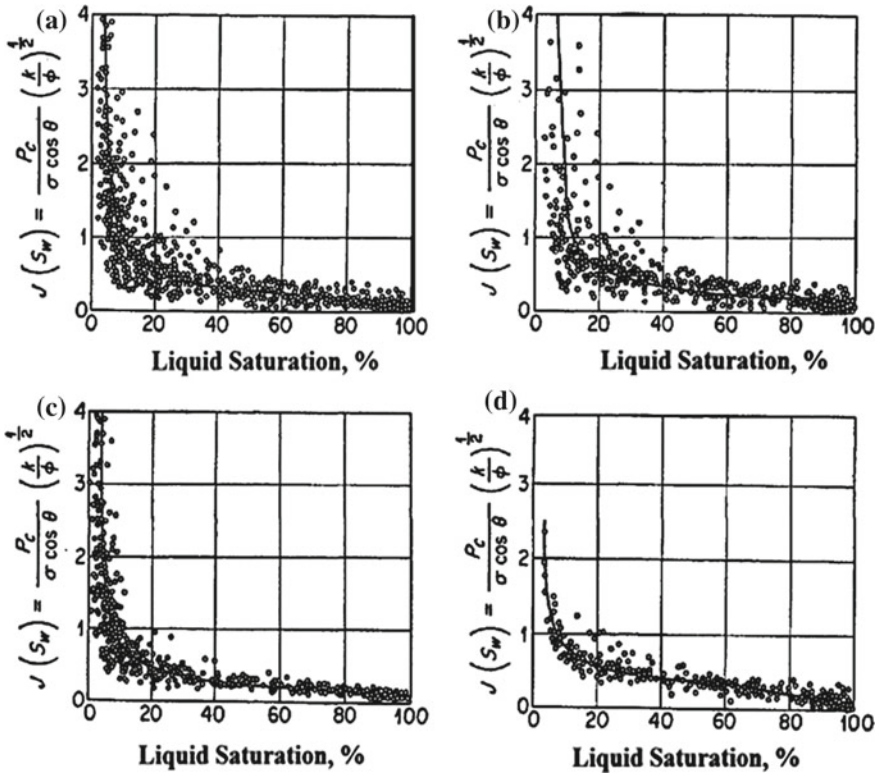


Fig. 5.13 J-function curve for **a** all core samples; **b** limestone samples; **c** dolomite samples; **d** microgranular limestone samples; **e** coarse-grained limestone samples. *Source* Amyx et al. (1960)

reservoir rock to other rocks that have similar rock type with differing permeability, porosity and wetting properties.

$$J(S_w) = C \cdot \frac{P_c}{\sigma} \sqrt{\frac{k}{\phi}} \tag{5.18}$$

where:

C = is constant.

For the same reservoir rock, this dimensionless equation helps to remove discrepancies in the P_c versus S_w curves for many cases and decrease them to a common curve.

Some writers changed Eq. 5.19 by including $\cos \theta$:

$$J(S_w) = \frac{P_c}{\sigma \cos \theta} \sqrt{\frac{k}{\phi}} \tag{5.19}$$

This equation is not unique, but it works better when the rocks are classified as to same rock types.

Example 5.1

Match of mercury injection capillary pressure data with porous diaphragm data.

A. Determine capillary pressure ratio?/

$$P_{cAH_g} / P_{cAw},$$

Giving the following data:

$$\sigma_{AH_g} = 480 \text{ Dynes/cm}$$

$$\sigma_{Aw} = 72 \text{ Dynes/cm}$$

$$\theta_{AH_g} = 140^\circ$$

$$\theta_{Aw} = 0^\circ$$

B. Aperture shape is very difficult. The curvature of the interface and aperture radius is not essentially depends on contact angles. Determine the capillary pressure ratio by applying the following correlation?

$$\frac{P_{cAH_g}}{P_{cAw}} = \frac{\sigma_{AH_g}}{\sigma_{Aw}}$$

Solution

(A)

$$\frac{P_{cAH_g}}{P_{cAw}} = \frac{\sigma_{AH_g} \cos \theta_{AH_g}}{\sigma_{Aw} \cos \theta_{Aw}} = \frac{480 \cos 140^\circ}{72 \cos 0^\circ}$$

$$\frac{P_{cAH_g}}{P_{cAw}} = 5.1$$

(B)

$$\frac{P_{cAH_g}}{P_{cAw}} @ \frac{\sigma_{AH_g}}{\sigma_{Aw}} = 480/72$$

$$\frac{P_{cAH_g}}{P_{cAw}} = 6.9$$

Example 5.2

Change laboratory scale data to reservoir conditions. State reservoir capillary pressure data by applying lab data.

Laboratory data:

$$\sigma_{AW} = 72 \text{ dynes}$$

$$\theta_{AW} = 0^\circ$$

Reservoir data:

$$\sigma_{oW} = 24 \text{ dynes/cm}$$

$$\theta_{oW} = 20^\circ$$

Solution

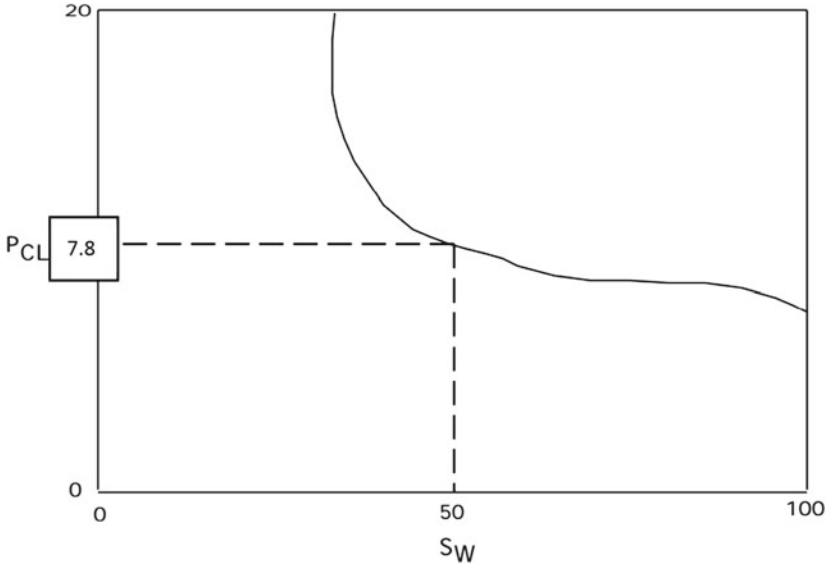
$$P_{cR} = \frac{(\cos \theta)_R}{(\cos \theta)_L} \cdot P_{cL}$$

$$P_{cR} = \frac{24(\cos 20)_R}{72(\cos 0)_L} \cdot P_{cL}$$

$$P_{cR} = 0.333 P_{cL}$$

Example 5.3

Using the laboratory capillary pressure curve capillary pressure curve given below, determining Water Saturation. Use $P_{cR} = 0.333 P_{cL}$, and assume the height of water saturation is 40 ft. above oil-water contact level. $\rho_o = 0.85 \text{ gm/cm}^3$, $\rho_w = 1.0 \text{ gm/cm}^3$.



Solution

$$P_{cR} = \frac{(\rho_w - \rho_o)}{144} \cdot h$$

$$P_{cR} = \frac{(1 - 0.85) \left(\frac{62.5 \text{ lbf}}{\text{ft}^3} \right) * 40}{144}$$

$$P_{cR} = 2.6 \text{ psi}$$

$$P_{cR} = 0.333 P_{cL}$$

$$P_{cL} = \frac{P_{cR}}{0.333}$$

$$P_{cL} = \frac{2.6}{0.333} = 7.8 \text{ psi}$$

From y-axis at $P_{cL} = 7.8$ psi move to the right horizontally to cross the capillary pressure curve and drop vertically to the x-axis, and read S_w value. $S_w = 50\%$.

Example 5.4

1. A goblet tube is positioned upright in a cup of water. The air-water interfacial tension is 72 dynes/cm with the contact angle is equal to 0° ?
 - (a) Determine the capillary increase of water in the tube if the tube radius is 0.01 cm.

- (b) Determine the difference in pressure across the interface of air-water in the tube.
2. 55 psi is the displacement pressure for a water saturated porcelain plate of air. What is the diameter of the biggest aperture in the porcelain plate? Use 72 dynes/cm with a contact angle is equal to 0 degrees?

Solution

- (1) $\sigma_{AW} = 72$ dynes
 $\rho_w = 1$ gm/cm³
 $g = 980$ dynes/gm
 $\theta = 0^\circ$

- (a) Capillary increase of water if radius is 0.01 cm

$$h = 2\sigma_{AW} \cos \theta / r \rho g$$

$$h = \frac{2(72) \cos 0}{(0.01)(1)(980)} = 14.69 \text{ cm}$$

- (b) Pressure drop across interface

$$P_c = p_a - p_w = r_w g h = (1.0)(980)(14.69)$$

$$P_c = 0.0142 \text{ atm} \left(14.696 \frac{\text{psi}}{\text{atm}} \right)$$

$$P_c = 0.209 \text{ psi}$$

- (2) $P_C = 2\sigma_{AW} \cos \theta / r$

$$P_C = 55 \text{ psi}$$

$$P_c = 55 \text{ psi} \left(\frac{\text{atm}}{14.696 \text{ psi}} \right) \left(\frac{1.0133 \times 10^6 \text{ dynes/cm}^2}{\text{atm}} \right)$$

$$P_C = 3.792 \times 10^6 \text{ psi}$$

$$r = 2\sigma_{AW} \cos \theta / P_c$$

$$r = \frac{2(72) \cos 0}{3.792 \times 10^6} = 3.797 \times 10^{-5} \text{ cm} \left(\frac{\text{in}}{2.54 \text{ cm}} \right)$$

$$r = 1.495 \times 10^{-5} \text{ in}$$

$$d = 2.99 \times 10^{-5} \text{ in}$$

References

- Amyx J, Bass D, Whiting R (1960) Petroleum reservoir engineering physical properties. McGraw-Hill, New York. ISBN: 9780070016002, 0070016003
- Archie GE (1950) Introduction to petrophysics of reservoir rocks. AAPG Bull 34:943–961
- Darling T (2005) Well logging and formation evaluation. Gulf Professional Publishing/Elsevier Inc.;
- de Lima OAL (1995) Water saturation and permeability from resistivity, dielectric, and porosity logs. Geophysics 60:1756–1764
- Hartmann D, Beaumont E (1999) Predicting reservoir system quality and performance. In: Beaumont EA, Forster NH (eds) AAPG treatise of petroleum geology, exploration for oil and gas traps, Chap. 9 (9-1 to 9-154)
- Jorden J, Campbell F (1984) Well logging I—rock properties, borehole environment, mud and temperature logging. Henry L. Doherty Memorial Fund of AIME, SPE: New York, Dallas
- Kolodziez Jr (1980) Analysis of pore throat size and use of the Waxman-Smiths equation to determine OOIP in Spindle Field, Colorado. SPE paper 9382 presented at the 1980 SPE annual technical conference and exhibition, Dallas, Texas
- Leverett MC (1941) Capillary behavior in porous solids. Pet Trans AIME 27(3):152–169
- Swanson BJ (1981) A simple correlation between permeability and mercury capillary pressures. J Pet Technol 2488–2504